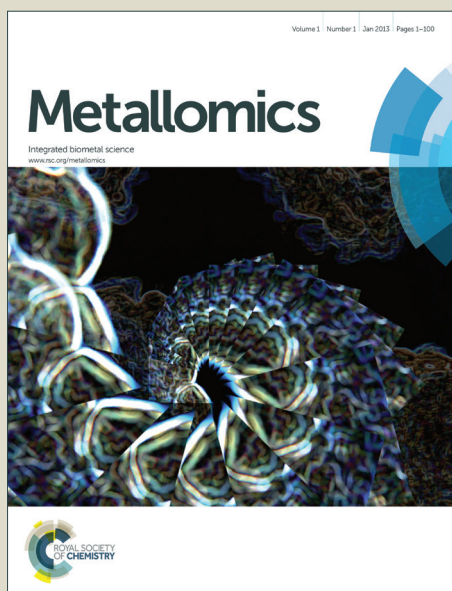


Metallomics

Accepted Manuscript



This is an *Accepted Manuscript*, which has been through the Royal Society of Chemistry peer review process and has been accepted for publication.

Accepted Manuscripts are published online shortly after acceptance, before technical editing, formatting and proof reading. Using this free service, authors can make their results available to the community, in citable form, before we publish the edited article. We will replace this *Accepted Manuscript* with the edited and formatted *Advance Article* as soon as it is available.

You can find more information about *Accepted Manuscripts* in the [Information for Authors](#).

Please note that technical editing may introduce minor changes to the text and/or graphics, which may alter content. The journal's standard [Terms & Conditions](#) and the [Ethical guidelines](#) still apply. In no event shall the Royal Society of Chemistry be held responsible for any errors or omissions in this *Accepted Manuscript* or any consequences arising from the use of any information it contains.

ARTICLE

EPR spectroscopy identifies Met and Lys residues that are essential for the interaction between CusB N-terminal domain and the metallochaperone CusF

Cite this: DOI: 10.1039/x0xx00000x

Received 00th January 2012,

Accepted 00th January 2012

DOI: 10.1039/x0xx00000x

www.rsc.org/

Aviv Meir,^a Adi Natan,^a Yoni Moskovitz,^a and Sharon Ruthstein^{a,*}

Copper plays a key role in all living organisms by serving as a cofactor for a large variety of proteins and enzymes involved in electron transfer, oxidase and oxygenase activities, and the detoxification of oxygen radicals. Due to its toxicity, a conserved homeostasis mechanism is required. In *E. coli*, the CusCFBA efflux system is one copper-regulating system and is responsible for transferring Cu(I) and Ag(I) out of the periplasm domain into the extracellular domain. Two of the components of this efflux system, the CusF metallochaperone and the N-terminal domain of CusB, have been thought to have significant roles in the function of this efflux system. Resolving the metal ion transport mechanism through this efflux system is vital for understanding metal- and multidrug-resistant microorganisms. This work explores one aspect of the *E. coli* resistance mechanism by observing the interaction between the N-terminal domain of CusB and the CusF protein, using electron paramagnetic resonance (EPR) spectroscopy, circular dichroism (CD), and chemical cross-linking. The data summarized here show that M36 and M38 of CusB are important residues for both the Cu(I) coordination to the CusB N-terminal domain and the interaction with CusF, and K32 is essential for the interaction with CusF. In contrast, K29 residue is less consequential for the interaction with CusF, whereas M21 is mostly important for the proper interaction with CusF.

Introduction

Transition metal ion concentrations must be highly regulated within all organisms to preserve cellular requirements and to avoid toxicity.¹⁻⁴ Copper is one of the most toxic metal ions; therefore, both eukaryotic and prokaryotic systems have developed sophisticated mechanisms for controlling copper homeostasis. Because copper is also used as an antibacterial agent,^{1,2,5-7} it is important to understand every detail of the bacteria cellular copper resistance mechanism. *E. coli* regulates its copper concentration through two regulating systems. The first system is cytoplasmatic and is mainly controlled by the Cu(I) metal sensor, CueR.^{8,9} CueR regulates the expression of two genes: *copA*, which encodes the Cu(I)-translocating P-type ATPase, and *cueO*, which encodes a Cu(I)-oxidizing multicopper oxidase. The second system is a periplasmatic four-component efflux system, CusCFBA.^{10,11} Three of the proteins in the system, CusA, CusB, and CusC, generate a metal efflux pump system that transports Cu(I) and Ag(I) from the cytoplasm environment to the extracellular domain. The fourth component

of this system, CusF, is specific to the Cus system and is essential for the copper efflux system.¹¹ Analysis of the different components of the Cus system showed that all Cus components are essential for full copper resistance.¹¹⁻¹³

The crystal structure of each component of this system has been resolved individually. The structure of CusA, CusB and the outer membrane factor, CusC, reveals a Cus A:B:C ratio of 3:6:3 of the monomeric units in the full CusCBA complex (see Figure 1A).^{14,15} The CusB structure of residues 89-385 suggests that each CusB monomer can be divided into four different domains, three of which are mostly β -strands, and the fourth is α -helical.¹⁶ The CusB-N terminal domain (CusBNT) region, which consists of the first 60 amino acids of the protein, is absent from the reported crystal structure. This region includes the three conserved Met residues (M21, M36, and M38) suggested to be the first metal-binding site of CusB, and may function as the entry point of the metal into the efflux complex.¹⁷ When this metal binding site is disrupted, a loss of metal resistance is observed, demonstrating the importance of

^a Department of Chemistry, Faculty of Exact Science, Bar Ilan University, Ramat Gan, Israel. 5290002

*Corresponding author: Dr. Sharon Ruthstein, sharon.ruthstein@biu.ac.il

the N-terminal domain of CusB to the efflux process.¹⁸ Molecular dynamic simulations on the first 50 amino residues suggest that CusBNT is largely disordered but adopts some structure upon metal binding.¹⁹

CusF, a unique part of the Cus efflux system, is a 102 amino acids protein, which folds into a five β -strands structure (Figure 1B).^{20,21} The exact role that the CusF protein plays in the metal resistance system has yet to be fully understood.¹² Padailla-Benavides and co-workers have successfully demonstrated a specific interaction between the CopA transporter extracellular domain and CusF.²² Moreover, the researchers showed that the metal transfer only occurred in one direction, from CopA to CusF. In a recent paper, Chacón et al. suggested by X-ray absorption spectroscopy, that the CusBNT-CusF interaction functions as a switch for the entire Cus efflux system and facilitates the metal transfer to the CusA component.²³ These findings suggest that in the periplasm, copper is transferred from CopA to CusF and then to the CusCBA complex through a direct and specific interaction (see Figure 1A). The interaction between CusF and CusBNT was studied by various physical methods such as isothermal titration calorimetry (ITC),²⁴ chemical cross-linking experiments,²⁵ and NMR,²⁵ all of which suggested a close and specific interaction between CusF and CusBNT upon metal coordination. NMR spectra also showed that the interaction between CusF and CusB is weak and that only about 38% of CusF is involved in a complex with CusB.²⁵ Despite this significant progress, the lack of structural data on the CusF-CusBNT complex has left many unanswered questions about the role of CusF and the CusF-CusBNT complex in the Cus efflux system.

Our goal herein is to gain additional structural information about the CusBNT-CusF interconnection using electron paramagnetic resonance (EPR) spectroscopy, and to identify key residues essential to this interaction. EPR has emerged as an excellent and highly sensitive tool for resolving protein-protein interactions.^{26,27} EPR is not crystallization dependent, is not limited by the protein size, and is sensitive to the molecular fluctuations that the protein undergoes upon metal/ligand and protein interactions. In addition, EPR can measure distances of up to 80 Å both between paramagnetic probes within the protein and between proteins.²⁷⁻³² The most common experiment for obtaining nanoscale structure information is the pulsed electron double resonance (PELDOR) experiment, also commonly known as the double electron-electron resonance experiment (DEER).³³⁻³⁵ Pulsed EPR experiments can measure nanometer distances between paramagnetic probes, and continuous wave (CW) EPR can reveal the dynamics of protein chains. EPR spectroscopy measurements of diamagnetic systems are performed using the site-directed spin labeling (SDSL) method.³⁶⁻³⁹ For SDSL, a stable nitroxide radical, the methanesulfonylthioate (MTSSL) spin-label, is attached via a disulfide bond to a cysteine residue. MTSSL is highly stable in solution, and usually causes minimal perturbations to the protein.^{40,41}

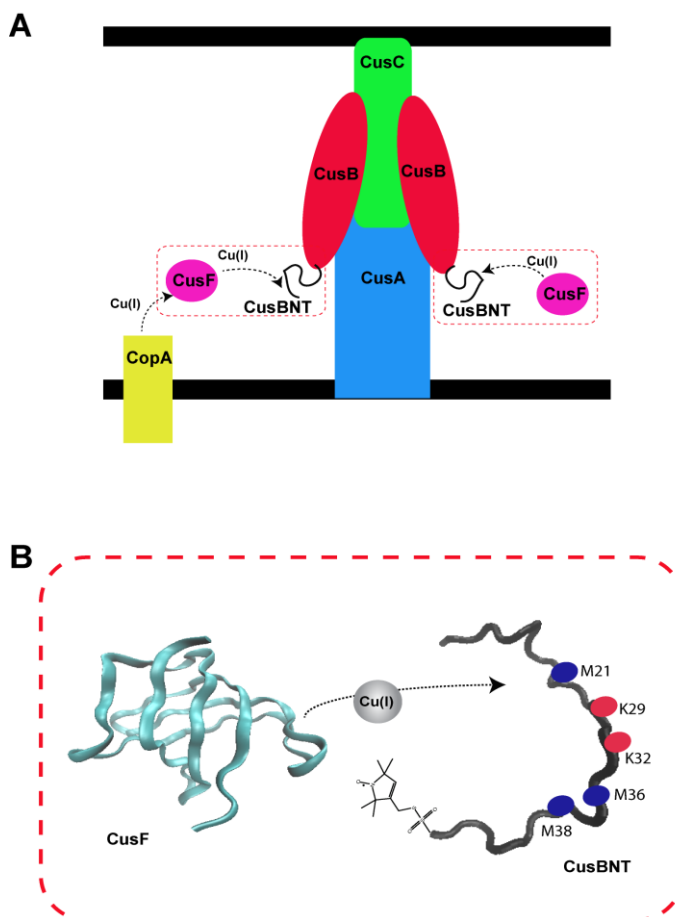


Figure 1: A. A schematic view presenting the CusCFBA periplasmic E.coli efflux system. B. Interaction between the CusB N-terminal (CusBNT) domain and the metallochaperone CusF (PDB: 2VB2⁴²). The CusBNT C-terminus was attached to the methanesulfonylthioate (MTSSL) spin-label using the site-directed spin-labeling (SDSL) method.

This study employs continuous wave (CW) and pulsed EPR spectroscopy along SDSL, chemical cross-linking, circular dichroism (CD), and mutagenesis to explore the interaction between the CusB N-terminal domain (the first 60 amino acids) and the CusF protein and to target key residues of CusBNT that participate in the copper transfer between these two domains. The role of the Met and Lys residues in both the copper coordination and the interaction with CusF are explored. Figure 1 shows a schematic model of the copper efflux pump system in the E.coli periplasm, and the assessed interaction between CusF and the spin-labeled CusB N-terminal domain (Figure 1B).

Materials and Methods

CusBNT cloning expression and Purification – The CusBNT gene was amplified from E. coli genomic DNA by PCR using primers containing specific CusBNT sequences and flanking regions that correspond to the expression vector sequences of pYTB12 (5' primer-GTTGTACAGAATGCTGGTTCATATGGAACCGCCTGCAG

1 AAAAAACG and 3' primer-
 2 GTCACCCGGGCTCGAGGAATTTTCTGAGTCGG
 3 GTCAATGCG). This amplicon was cloned into the pYTB12
 4 vector using the free ligation PCR technique.⁴³ This construct,
 5 which encodes for the fusion protein composed of CusBNT,
 6 intein and a chitin-binding domain, was transformed into the E.
 7 coli strain BL21 (DE3). The CusB construct was expressed in
 8 BL21 cells, which were grown to an optical density of 0.6-0.8 at
 9 600 nm and were induced with 1 mM isopropyl- β -D-
 10 thiogalactopyranoside (CALBIOCHEM) for 18 h at 18°C. The
 11 cells were then harvested by centrifugation, and the pellets were
 12 subjected to three freeze-thaw cycles. The pellet was
 13 resuspended in lysis buffer (25 mM Na₂HPO₄, 150 mM NaCl,
 14 and 20 μ M PMSF; pH 7.5). The cells were sonicated by 6 bursts
 15 of 1 minute each with a 1 minute cooling period between each
 16 burst (65% amplitude). After sonication, the cells were
 17 centrifuged, and the soluble fraction of the lysate was passed
 18 through a chitin bead column (New England Biolabs), allowing
 19 the CusB fusion to bind to the resin via its chitin-binding
 20 domain. The resin was then washed with 30-column volumes of
 21 lysis buffer. To induce the intein-mediated cleavage, the beads
 22 were incubated in 50 mM dithiothreitol (DTT), 25 mM
 23 NaH₂PO₄, and 150 mM NaCl at pH=8.9, for 40 h at room
 24 temperature. CusB was then collected in elution fractions and
 25 analyzed by SDS PAGE (19% tricine) and mass spectroscopy.
 26 The mass of the protein was confirmed using a MALDI-TOF
 27 MS-Autoflex III-TOF/TOF mass spectrometer (Bruker,
 28 Bremen, Germany) equipped with a 337 nm nitrogen laser.

31 **CusF cloning expression and Purification** – The CusF gene was
 32 amplified from E. coli genomic DNA by PCR using primers
 33 containing specific CusF sequences and flanking regions
 34 (underlined) that corresponded to the expression vector
 35 sequences of pET28a (5' primer
 36 GTTAACTTTAAGAAGGAGATATACCATGTTTGTAGTCTG
 37 TTT ACCGTTATTGGC and 3' primer-
 38 GTCATGCTAGCCATATGCTAG AATCTTACTGGC
 39 TGACTTTAATATCCT). This amplicon was cloned into a
 40 pET28a vector using the free ligation PCR technique.⁴³ The
 41 CusF-pET28a construct was then transformed into E. coli BL21
 42 cells. The cells were grown to an optical density of 0.6-0.8 at
 43 600 nm and induced with 1 mM isopropyl- β -D-
 44 thiogalactopyranoside (CALBIOCHEM) for 3 h at 37°C. The
 45 cells were then harvested by centrifugation, and the pellets were
 46 subjected to three freeze-thaw cycles. The pellet was
 47 resuspended in NPI-10 buffer (300 mM NaCl, 50 mM
 48 NaH₂PO₄·2H₂O, and 10 mM imidazole; pH=8.0). The cells
 49 were sonicated by 6 bursts of 1 minute each with a 1 minute
 50 cooling period between each burst (65% amplitude). After
 51 sonication, the cells were centrifuged, and the soluble fraction
 52 of the CusF lysate was purified on Ni-NTA beads according to
 53 the manufacturer's protocol (Macherey Nagel). The elution
 54 fractions were confirmed by tricine SDS-PAGE.⁴⁴

CusBNT spin labeling - 0.25 mg of S-(2,2,5,5-tetramethyl-2,5-
 dihydro-1H-pyrrol-3-yl)methyl methanesulfonylthioate
 (MTSSL, TRC) dissolved in 15 μ l dimethyl sulfoxide (DMSO,
 Bio lab) was added to 0.75 ml of 0.2 mM protein solution (100-
 fold molar excess of MTSSL). The protein solution was then
 vortexed overnight at 4°C. The free spin label was removed by
 several dialysis cycles over 4 days. The mass of the spin-labeled
 protein was confirmed using a mass spectrometer, and the
 concentration was determined by a Lowry assay.⁴⁵

Addition of the metal ion: Cu(I) (Tetrakis (acetonitrile) copper (I)
 hexafluorophosphate (Aldrich)) was added to the protein solution
 under nitrogen gas to preserve anaerobic conditions. No Cu(II) EPR
 signal was observed at any time.

Glutaraldehyde cross-linking - Treatment with glutaraldehyde
 was conducted by mixing 50 μ g (20 μ l) of interacting protein in
 a 20 mM (70 μ l) sodium phosphate and 0.15 M NaCl solution at
 pH=8 (PBS X10), which was then reacted with 10 μ l of
 glutaraldehyde solution, incubated and shaken for 10 minutes at
 37°C. The reaction was terminated by the addition of 10 μ l of 1
 M Tris-HCl at pH=8.

Table 1 lists the CusBNT mutants studied in this research.

Table 1: CusBNT mutants studied in this research

Name	Mutation
CusBNT1	WT-CusBNT
CusBNT2	CusBNT-C61R1
CusBNT2_M21I	CusBNT2+M21Ile
CusBNT2_M38I	CusBNT2+M38Ile
CusBNT2_M21I_M38I	CusBNT2+M21Ile+M38Ile
CusBNT2_M36I_M38I	CusBNT2+M36Ile+ M38Ile
CusBNT2_M21I_M36I	CusBNT2+M21Ile+M36Ile
CusBNT2_M21I_M36I_M38I	CusBNT2+M21Ile+M36Ile+ M38Ile
CusBNT2_K29A	CusBNT2+K29A
CusBNT2_K32A	CusBNT2+K32A
CusBNT2_K29A_K32A	CusBNT2+K29A+K32A

¹ R1 represents the S-(2,2,5,5-tetramethyl-2,5-dihydro-1H-pyrrol-3-
 yl)methyl methanesulfonylthioate (MTSSL) spin-label attached to the
 cysteine residue.

EPR CW-EPR (continuous wave EPR) spectra were recorded
 using an E500 Elecsys Bruker spectrometer operating at 9.0-9.5
 GHz. The spectra were recorded at room temperature using a
 microwave power of 20.0 mW, modulation amplitude of 1.0 G,
 time constant of 60 ms, and receiver gain of 60.0 dB. The
 samples were measured in 0.8 mm capillary quartz tubes
 (VibroCom).

A constant-time four-pulse DEER experiment with $\pi/2(\text{vobs})-$
 $\tau_1-\pi(\text{vobs})-t'-\pi(\text{vpump})-(\tau_1+\tau_2-t')-\pi(\text{vobs})-\tau_2(\text{vobs})-\tau_2$ -echo
 was performed at (80 \pm 0.5 K) on a Q-band Elecsys E580
 (equipped with a 2 mm probe head, bandwidth = 220 MHz). A
 two-step phase cycle was employed on the first pulse. The echo

was measured as a function of t' , while τ_2 was kept constant to eliminate relaxation effects. The observer pulse was set 60 MHz higher than the pump pulse. The observer $\pi/2$ and π pulses had a length of 40 ns, as did the π pump pulse; the dwell time was 20 ns. The observer frequency was 33.82 GHz. The power of the 40 ns π pulse was 20.0 mW. The samples were measured in 1.6 mm capillary quartz tubes (Wilmand). The data were analyzed using the DeerAnalysis 2013 program and Tikhonov regularization.⁴⁶ The regularization parameter in the L curve was optimized by examining the fit of the time-domain data. The data presented in this manuscript have undergone 3D homogeneous background subtraction.

CD Circular dichroism (CD) measurements were conducted using a Chirascan spectrometer (Applied Photophysics, UK). Measurements were performed at room temperature in a 1 mm optical path length cell, and the spectra were recorded from 270–190 nm with a step size and a bandwidth of 0.5 nm. The CD signal was averaged for 10 sec every 2 nm. There were 3 scans.

Results

Cu(I) coordination to CusB N-terminal domain (CusBNT)

CusBNT and CusF lack cysteine residues. To explore the molecular structure of CusBNT using EPR and SDS, we inserted a cysteine into the C-terminus of CusBNT and then labeled the protein with an MTSSL spin-label. The SDS gel and mass spectrometry results of a non-labeled and a labeled CusBNT2 protein are presented in Figure 2, indicating 100% spin-labeling.

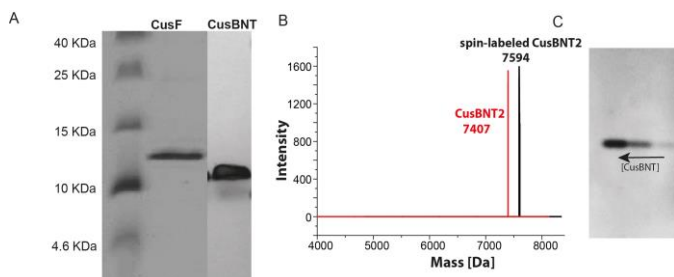


Figure 2: A. SDS-PAGE tricine (19%) gel of CusF and CusBNT, confirming purified protein. B. MALDI-mass spectrum of CusBNT and spin-labeled CusBNT. C. Native tricine gel of CusBNT, confirming the presence of a purified monomer of CusBNT.

Figure 3 shows the CW-EPR spectra of CusBNT2 at various concentrations. The CW-EPR spectra recorded at room temperature are characteristic of the fast dynamics of the nitroxide spin-label, resulting in an isotropic spectrum, and the spectra shows characteristic signals of an exchange interaction, marked by arrows in Figure 3. The CW-EPR spectra are similar for various concentrations, as low as 0.025 mM. This result indicates both a close interaction between CusBNT monomers and the possible formation of dimers or aggregates. Hence, we ran a native gel in the presence of various concentrations of

CusBNT. The native tricine gel confirmed that the CusBNT existed only as monomers and that a non-covalent bond was formed (see Figure 2C). Moreover, concentration-dependent oligomerization was not observed in the gel. Therefore, we believe that CusBNT monomers closely interact with each other via hydrogen or electrostatic bonds, without forming a stable bound complex.

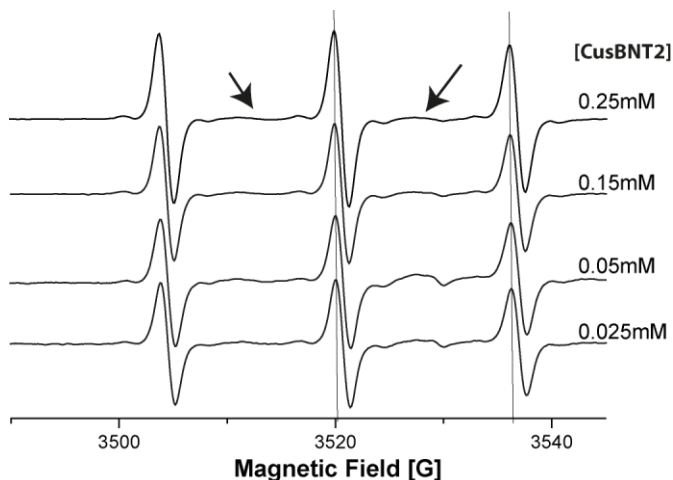


Figure 3: CW-EPR spectra of CusBNT2 at various concentrations. The arrows mark the characteristic signals caused by the exchange interaction between two paramagnetic centers.

When exploring the role of the three methionine residues in the Cu(I) coordination of CusBNT, we expressed several mutants (see Table 1): M21Ile (CusBNT2_M21I), M38Ile (CusBNT2_M38I), Met21Ile_Met38Ile (CusBNT2_M21I_M38I), Met36Ile_Met38Ile (CusBNT2_M36I_M38I), Met21Ile_Met36Ile (CusBNT2_M21I_M36I), and Met21Ile_Met36Ile_Met38Ile (CusBNT2_M21I_M36I_M38I). We chose to mutate methionine to isoleucine to minimize possible structural changes in the protein upon mutation. We followed the changes in the line shape of the CW-EPR spectra of CusBNT2 and the various mutants. Figure 4A shows the CW-EPR spectra of CusBNT2 at various Cu(I) concentrations. For CusBNT2, a continuous decrease in the hyperfine coupling (a_N) upon Cu(I) coordination was observed. The change in the hyperfine values of CusBNT2 and of the various mutants is plotted in Figure 4B. The error in the evolution of the hyperfine coupling is 0.1 G. For CusBNT2, a reduction from 15.1 G at $[\text{Cu(I)}]=0$ to 14.0 G at $[\text{Cu(I)}]/[\text{CusBNT2}]=5$ is observed. Below that given copper concentration, no reduction in the EPR signal was observed, confirming that no protein aggregates formed. The reduction in the hyperfine values as a function of copper coordination suggests that the spin-label attached to the C-terminus of CusBNT points toward a more hydrophobic environment upon Cu(I) coordination. The continuous decrease in the hyperfine value even at a 5:1 ratio of $[\text{Cu(I)}]/[\text{CusBNT2}]$ does not indicate that there are five copper ions coordinated to one CusBNT monomer. Instead, this finding shows that the affinity of the metal ion to CusBNT is relatively low; ITC experiments

previously suggested that the affinity was in the range of a few μM .²⁴ Hence, a high concentration of copper is required for all proteins to be coordinated to one copper ion. At very high copper concentrations > 10 $[\text{Cu(I)}]/\text{CusBNT}$, protein aggregation began to appear, manifested by a reduction in the EPR signal; this finding suggests that at this concentration, more than one copper ion is linked to a CusBNT monomer. Mutation of Met21Ile almost did not affect the copper coordination to CusBNT, and a similar pattern appeared in the CW-EPR line shape upon copper coordination. However, the mutations of Met36 and Met38, did affect the copper coordination, and the change in the hyperfine coupling value as a function of $[\text{Cu(I)}]$ was smaller, as presented in Figure 4B. Triple mutations of all three methionine residues nearly did not change the hyperfine coupling upon copper coordination, suggesting that copper cannot coordinate CusBNT without the presence of these methionine residues. This result also supports the in-cell experiments, which indicate that mutations of these methionine residues affect copper resistance.¹⁸ The differences in the hyperfine coupling values for all various mutants suggest that M36I and M38I have the largest effect on copper coordination to CusBNT, which is least affected by the M21I mutation.

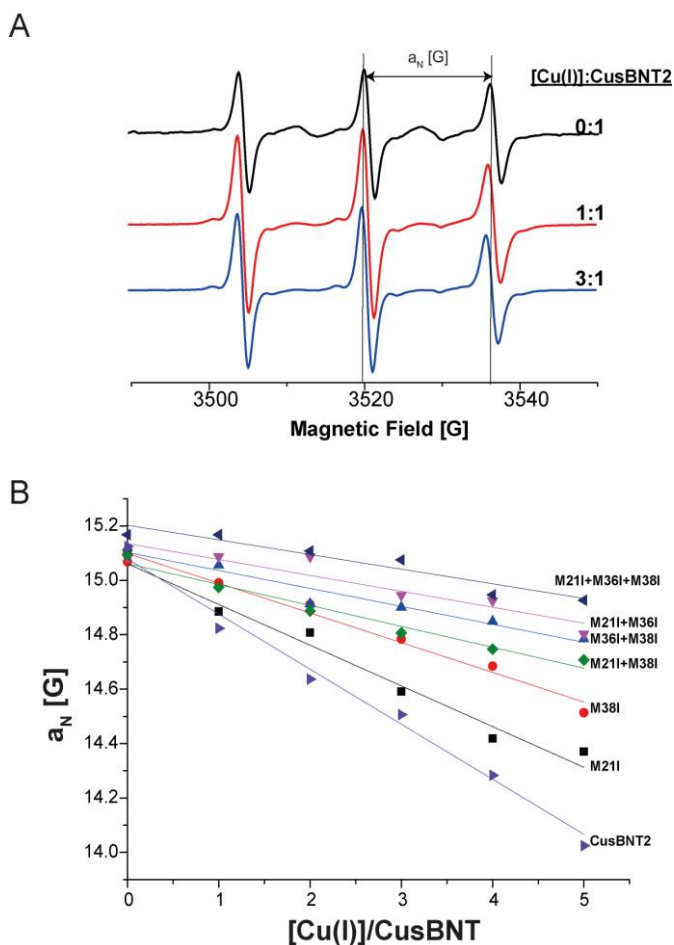


Figure 4: A. CW-EPR spectra of CusBNT2 at various $[\text{Cu(I)}]$ concentrations. B. The change in the hyperfine value, a_N , for CusBNT2 and the various CusBNT2 mutants as a function of $[\text{Cu(I)}]$ concentration.

The role of the three methionine residues in the interaction with CusF

To further explore the role of the methionine residues involved in the interaction with CusF, we fully expressed CusF, and its SDS gel is shown in Figure 2A. The incorporation of CusF into the CusBNT solution did not change the hyperfine value (a_N) obtained from the EPR spectra line shape, as presented in Figure 5A. When adding Cu(I) to the solution, the trend was similar to the one observed without the presence of CusF, showing a reduction in the hyperfine value (Figure 5B). The EPR spectrum was identical whether apo-CusF was added to the Cu(I)-CusBNT2 solution, or apo-CusBNT was added to the Cu(I)-CusF solution (Figure 5A). This proposes that the EPR spectrum was acquired after a steady state was reached, and that the affinity of Cu(I) to CusBNT is higher than its affinity to the CusF metallochaperone. The M21I mutation resulted in a similar reduction of the hyperfine value as a function of $[\text{Cu(I)}]$ in the presence of CusF, compared to the hyperfine value in its absence (Figure 4B). Double mutations involving M36I or M38I strongly affected the copper coordination to CusBNT, and a slight reduction in the hyperfine value was observed. Figures 4 and 5 suggest that the hyperfine value is insensitive to the presence of CusF, since the trend in the hyperfine value reduction for the various mutants as a function of Cu(I) coordination is similar in the presence and absence of CusF, within the experimental error ($\pm 0.1\text{G}$).

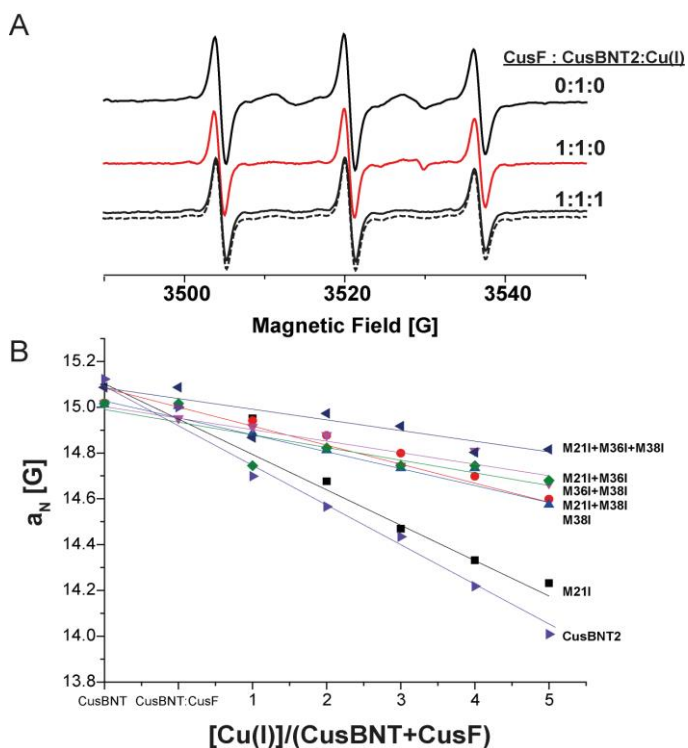


Figure 5: A. CW-EPR spectra of CusBNT2 and CusBNT2 in the presence of CusF, and in the presence of Cu(I) and CusF (dashed line: CusF was added to a solution of Cu(I)-CusBNT2, solid line: CusBNT2 was added to a solution of Cu(I)-CusF). B. Change in the hyperfine value, a_N , of CusBNT2 and the various CusBNT2 mutants, in the presence of CusF, and as a function of $[\text{Cu(I)}]$ concentration.

The hyperfine value was not the only parameter affected by the Cu(I) coordination. A close examination of the CW-EPR spectra also revealed a reduction of the exchange interaction in the presence of Cu(I) for CusBNT2 (see Figure 6A), where a mutation of the methionine residues also reduced the interaction between CusBNT monomers. Figure 6A shows the CW-EPR spectra of CusBNT2, CusBNT2_M21I, and CusBNT2_M21I_M36I_M38I. In these spectra, the line shapes corresponding to exchange interactions appear for CusBNT2; these characteristics are not observed in CusBNT2_M21I_M36I_M38I. We followed the change in the I₂/I₁ ratio for the various mutants as a function of Cu(I) coordination (Figure 6B). For both CusBNT2 and CusBNT2_M21I, a reduction in the exchange interaction appeared (reduction in the I₂/I₁ value), suggesting that the presence of Cu(I) separates the CusBNT monomers and decreases the interaction between them. However, double mutations involving M36I or M38I can already separate the CusBNT monomers even in the absence of copper ions. This finding suggests that the methionine residues play a role in the interaction between the CusBNT monomers. At higher Cu(I) concentrations, a smaller increase in the exchange interaction appears for CusBNT2_M38I and CusBNT2_M36I_M38I, this might be due to some increase in CusBNT aggregation due to the high copper concentration. The addition of CusF to CusBNT2 reduced the exchange interaction, observed in Figure 6C, indicating that CusF itself can separate CusBNT monomers. However, the presence of Cu(I) facilitated the separation between the CusBNT2 monomers. The addition of CusF to a CusBNT2_M21I solution revealed a larger reduction in the exchange interaction when compared the one for CusBNT2. This result suggests that the M21 residue might participate in the interaction between CusBNT and CusF.

The CW-EPR spectra indicate that the methionine residues are important not only for copper coordination, but also for preserving the proper folding structure of CusBNT, allowing it to interact in a specific manner with both companion CusBNT monomer, and the CusF protein. These results show that M36 and M38 residues are significant for both the Cu(I) coordination and the CusBNT-CusF interaction.

To further explore the conformational changes that CusBNT2 and CusF experience upon interaction, double electron-electron resonance (DEER) experiments were conducted. We performed DEER experiments on CusBNT2 alone and on CusBNT2 in the presence of Cu(I) and CusF (1:1:3 CusBNT2:CusF:Cu(I), respectively). The DEER signals are presented in Figure 7. The presence of a dipolar interaction between spin-labels confirms that the two CusBNT2 monomers are in close proximity. The distance distribution (inset in Figure 7) shows a distribution of 2.5 ± 0.6 nm between the two spin labels attached to the C-terminus of CusBNT. The addition of CusF and Cu(I) removed the dipolar interaction between the spin labels, and the DEER signal was characterized just by a homogeneous exponential decay. The DEER signal confirmed that in the presence of CusF

and Cu(I), CusBNT2 monomers are not in close proximity to each other. This finding is consistent with the CW-EPR data, where a reduction in the I₂/I₁ value was observed.

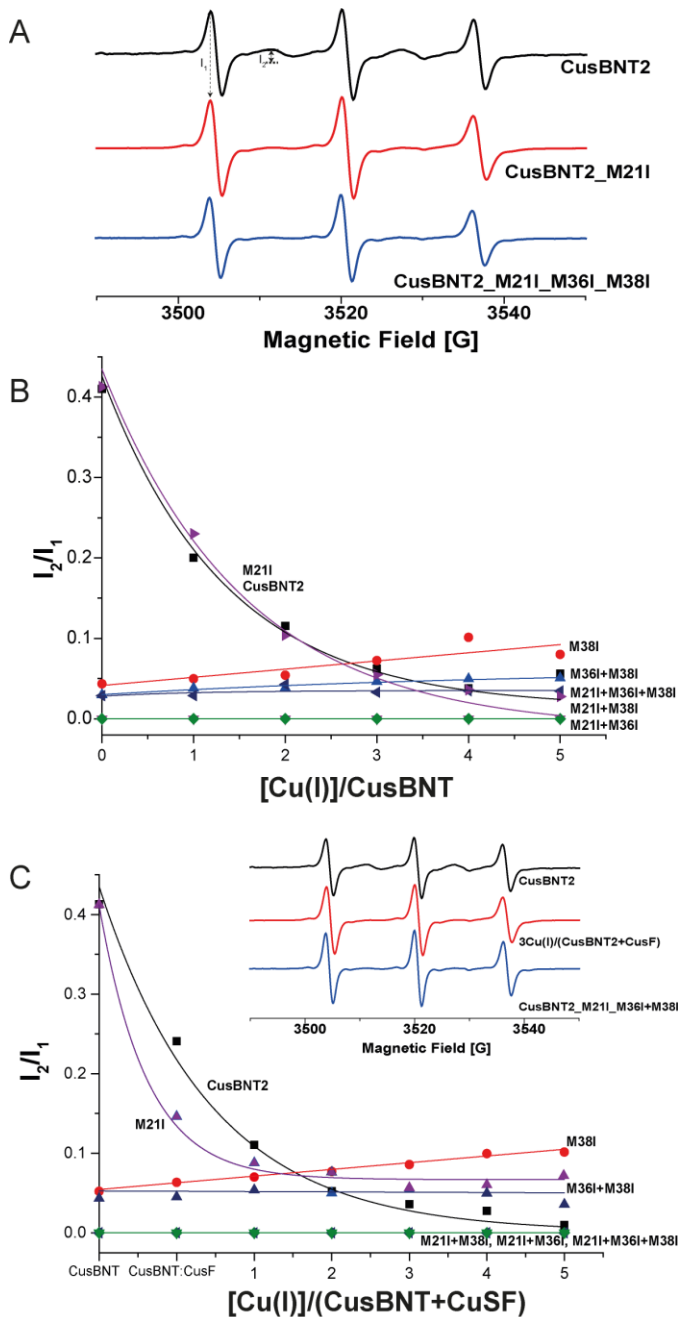


Figure 6: A. CW-EPR spectra of CusBNT2, CusBNT2_M21I, and CusBNT2_M21I_M36I_M38I. Change in the extent of the exchange interaction value, I₂/I₁, of the various CusBNT2 mutants (B) as a function of [Cu(I)] concentration, and (C) in the presence of CusF and [Cu(I)].

We also performed chemical cross-linking experiments on CusBNT in the presence of CusF and Cu(I). Figure 8A presents the SDS gels. It is clear that without the cross-linker, no complexes are formed between CusBNT2 monomers and

CusF-CusBNT2 even in the presence of Cu(I). In the presence of a cross-linker, no dimers are formed between two CusBNT monomers, suggesting that the lysine residues of two different CusBNT2 monomers are not close enough to each other to form a stable complex. However, in the presence of CusF, with no dependency on Cu(I), stable complexes do form, as indicated in the gel; this result suggests a close interaction between CusF and CusBNT2 through the lysine residues, as was previously proposed.²⁵ This experiment also shows that the interaction between CusBNT and CusF can occur even in the absence of the Cu(I) ion. Mutation of either of the methionine residues significantly affects the crosslinking, as observed in Figure 8B, and no cross-links are formed between CusBNT and CusF. This finding indicates that the methionine segments are important for preserving a specific folding structure of CusBNT. To support these data, CD measurements were performed on both CusBNT2 and CusBNT2_M21I_M36I_M38I (see Figure 9). The CD structure of CusBNT2, characterized by negative peaks at 200 nm and 235 nm, suggests that the secondary structure is a mix of α -helices, β -sheets and disordered segments. Conversely, the CD of CusBNT2_M21I_M36I_M38I was characterized by a negative peak at 215 nm, suggesting a larger contribution of β -sheets to the secondary structure.

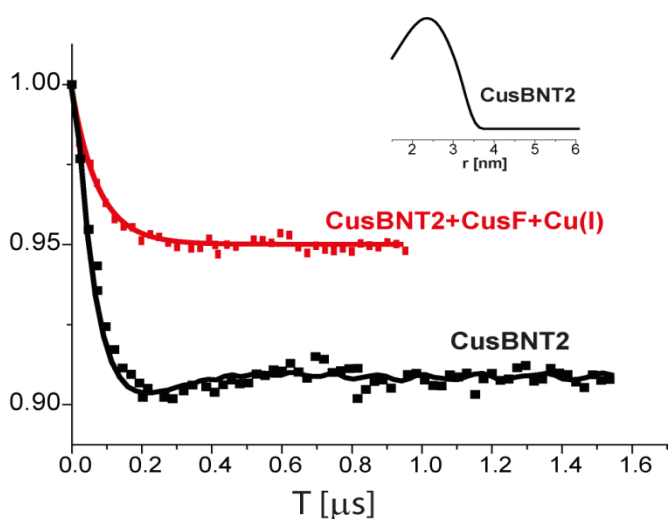


Figure 7: Q-band DEER signals, measured at 80K, of CusBNT2, and CusBNT2+CusF+3Cu(I). The inset shows the distance distribution obtained from the CusBNT2 DEER signal.

The role of lysine residues in the CusBNT-CusF interaction

K29 and K32 were previously suggested to play a role in the interaction with CusF.²⁵ Hence, we observed the changes in the CW-EPR spectra of CusBNT2_K29A, CusBNT2_K32A, and CusBNT2_K29A_K32A (see Table 1) as a function of copper coordination and the interaction with CusF. Figure 10A shows the CW-EPR spectra of CusBNT2, CusBNT2_K29A, CusBNT2_K32A, and CusBNT2_K29A_K32A. It is clear that mutations of the lysine residues removed the exchange interaction observed for CusBNT2, suggesting that CusBNT folds differently in the presence of these mutations and that they

spread two CusBNT monomers apart. Observing the change in the I2/I1 ratio for these mutants (Figure 10B) showed that there is nearly no change in this ratio as a function of copper and CusF coordination. We also observed the change in the hyperfine interaction (Figure 10C), which showed that although a strong reduction in the hyperfine value is noted for CusBNT2 in the presence of CusF and copper, only a minor reduction of approximately 0.3-0.4 G from [Cu(I)]=0 up to [Cu(I)]/(CusBNT+CusF)=4 for CusBNT2_K29A, CusBNT2_K32A, and CusBNT2_K29A_K32A is noted in the hyperfine value. The K32A mutation has the greatest effect on the copper coordination. Since lysine residues are not directly coordinated with the copper ion, the EPR spectra suggest that mutations of lysine residue might affect the structure of CusBNT, and by this interfere with the Cu(I) coordination to CusBNT. A CD spectrum of CusBNT2_K29A_32A is presented in Figure 9, showing some differences in the secondary structure of these mutants, confirming our observation. Chemical cross-linking experiments on CusBNT2_K29A, CusBNT2_K32A, and CusBNT2_K29A_K32A are presented in Figure 8C. The K29A (CusBNT2_K29A) mutation did not interfere with the formation of the CusBNT-CusF complex. However, the K32A (single K32A or double mutation of K29A and K32A) disrupted the formation of a complex between CusBNT and CusF, indicating that K32 is an important residue for the interaction between CusF and CusBNT.

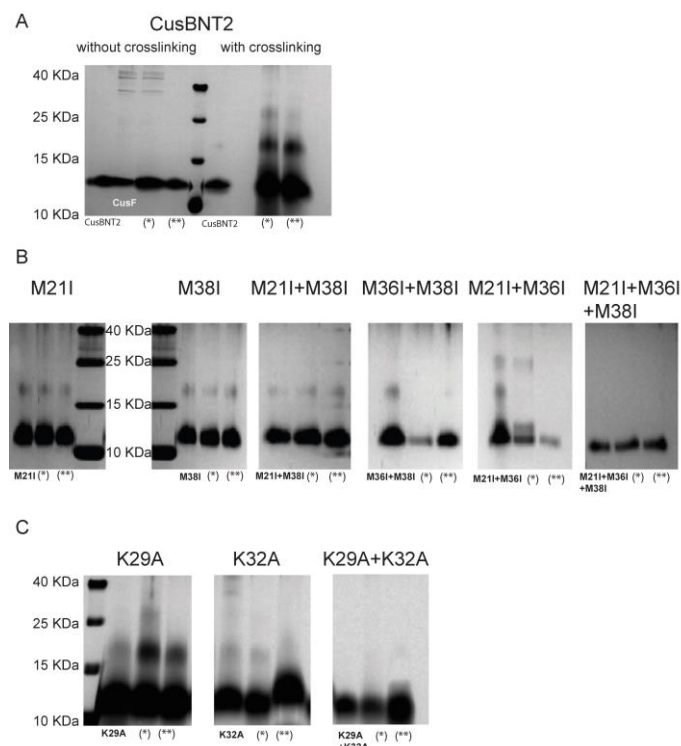


Figure 8: Chemical cross-linking SDS-PAGE tricine (19%) gel, showing the following: A. interactions between CusBNT2 and CusF, (*) marks CusBNT2+CusF and (**) marks CusBNT2+CusF+Cu(I) B. CusBNT2 methionine mutations in the presence of CusF (*), and in the presence of CusF+Cu(I) (**), and C. CusBNT lysine mutations.

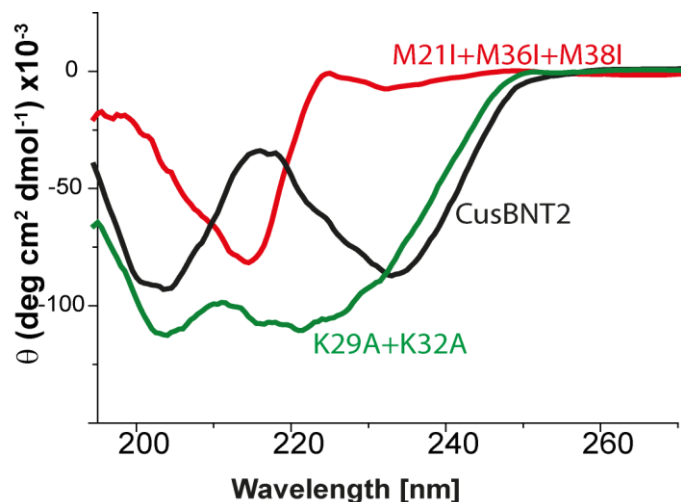


Figure 9: CD spectra of apo-CusBNT2, apo-CusBNT2_M21I_M36I_M38I, and apo-CusBNT2_K29A_K32A.

Discussion

This study aimed to provide molecular structural insight into two individual important components of the E.coli Cus efflux system: the N-terminal domain of the CusB (CusBNT) protein and the metallochaperone CusF. Earlier studies indicated the importance of these two domains to the functionality of the Cus efflux system. The EPR data show that CusBNT monomers prefer to be in close proximity to each other, the addition of CusF separates CusBNT monomers, and the addition of Cu(I) facilitates this separation. This finding explains the NMR and ITC results, which only successfully resolved the interaction between CusF and CusBNT in the presence of Cu(I).^{18,25} EPR is much more sensitive than NMR, and can thus resolve even weak interaction between proteins, with only about 20% of the dissolved proteins in a complex.^{47,48} In the presence of a metal ion, the amount of interacting proteins is higher, and can be resolved by less sensitive techniques. A close interaction between CusF and CusB was also observed in the chemical cross-linking experiments with and without Cu(I). The CW-EPR spectra indicate that the methionine residues are important not only for copper coordination but also for preserving the proper folding structure of CusBNT, allowing it to interact in a specific manner with both the companion CusBNT monomer and the CusF protein. This role has been confirmed by the CD spectra, which showed that mutation of all three methionine residues unfolds the protein, resulting in a disordered CusBNT structure. Chemical cross-linking showed that in the presence of any of the methionine mutants, no cross-linking between CusBNT and CusF occurred. Moreover, M36 and M38 were important for copper coordination and the interaction with CusF. M21, however, may not be essential to copper coordination but may be significant for the CusF-CusBNT interaction and for the metal transfer mechanism. X-ray absorption spectroscopy studies showed that all three methionine residues are required

for Cu(I) coordination.¹⁸ The group of Franz et al. suggested that three methionine residues are required to form a high affinity Cu(I) binding site, however, lower affinity Cu(I) binding site can be formed with only two methionine residues.^{49,50} As previously noted, the EPR measurements are performed after a steady state is reached, thus we believe that Cu(I) can still coordinate to CusBNT_M21I through a coordination site containing only two methionine residues. The affinity to this site might be lower; however, EPR cannot detect it and report on the affinity of Cu(I). This is also consistent with the previous ITC results. ITC was used to determine the ability of the CusB mutants, M21I, M36I, and M38I, to bind Ag(I) *in vitro*.¹⁸ The M21I mutant of CusB showed a 10-fold reduction in binding affinity for Ag(I) compared with that for wild-type CusB, with a dissociation constant of 0.2 μ M. The M36I and M38I mutants of CusB showed no specific binding to Ag(I). Considering Ag(I) and Cu(I) have a similar charge and nature, these results also demonstrate the importance of M36 and M38 for metal coordination, and the lesser significance of M21 to the coordination of the metal. Cell experiments have shown that cells with the M21I, M36I, and M38I mutants of CusB did not grow.¹⁸ This result suggests that even if M21I has no significant role in metal coordination, it still might be essential for metal transfer and thus essential for the resistance of the cell to copper ions, as was also observed in the EPR experiments of this study.

Herein, we have also shown using both EPR measurements and chemical cross-linking that the K32A (CusBNT2_K32A, CusBNT2_K29A_K32A) mutant disrupted the formation of a complex between CusBNT and CusF, indicating that K32 is a key residue in the interaction between CusF and CusBNT. It is interesting that both mutations of hydrophobic residues, such as methionine residues, and hydrophilic residues (lysine) affect the structure of CusBNT and by this remove the interaction between two CusBNT monomers and the interaction between CusBNT and CusF.

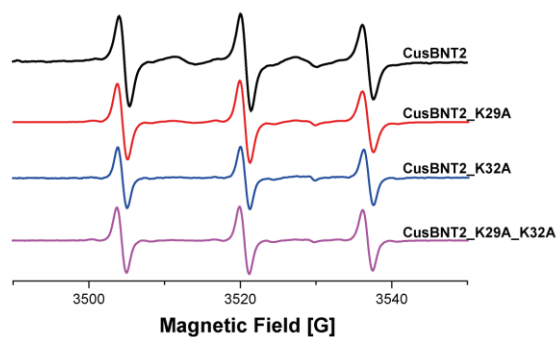
Conclusions

A combination of EPR spectroscopy, CD, and chemical cross-linking experiments has successfully shed some light on the interaction between the CusF metallochaperone and the N-terminal domain of the CusB protein. M36 and M38 of CusBNT were found to be essential residues both for Cu(I) coordination and for the interaction with the CusF, and K32 were found to be important for CusF-CusBNT interaction. In contrast, K29 is less consequential for the interaction with CusF protein, while M21 is mostly important for the CusF-CusBNT interaction. This research provides useful information on the interconnection between CusBNT and CusF, and on the key residues that are controlling the Cu(I) regulation in the E.coli periplasm.

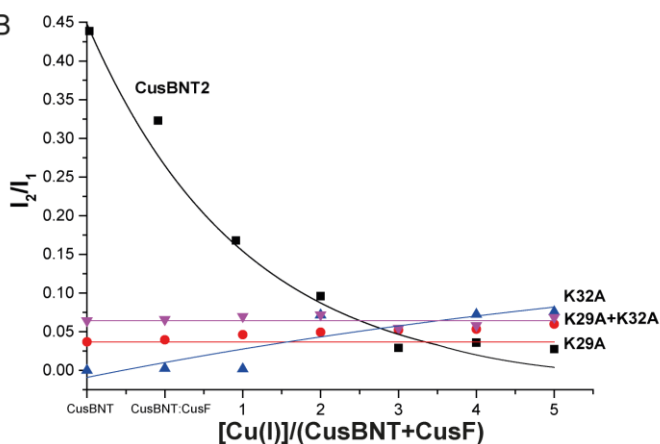
Acknowledgment

This study was supported by MC CIG, grant no. 303636. The Eleksys E580 Bruker EPR spectrometer was partially supported by the Israel Science Foundation, grant no. 564/12.

A



B



C

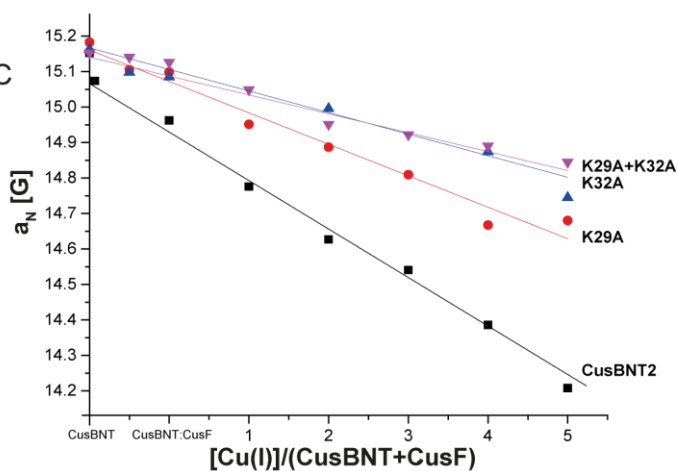
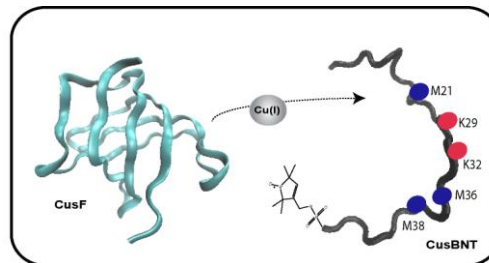


Figure 10: A. CW-EPR spectra of CusBNT2, CusBNT2_K29A, CusBNT2_K32A, and CusBNT2_K29A_K32A. B. Change in the extent of the exchange interaction value, I_2/I_1 , of the various CusBNT2 Lys mutants as a function of $[Cu(I)]$ concentration, and in the presence of CusF and $[Cu(I)]$. C. Change in the hyperfine value, a_N , of the various CusBNT2 mutants in the presence of CusF and as a function of $[Cu(I)]$ concentration.

Graphical abstract

Methionine and Lysine residues are important for preserving the structure of CusB N-terminal domain and for the interaction with CusF.



References

- 1 (1) S. Silver, *FEMS microbiology reviews* 2003, **27**, 341-353.
- 2 (2) S. Silver, L.T. Phung, and G. Silver, *J. Ind. Microbiol.*
- 3 *Biotechnol.* 2006, **33**, 627-534.
- 4 (3) J.L. Burkhead, K.A. Gogolin Reynolds, S.E. Abdel-Ghany,
- 5 C.M. Cohu, and M. Pilon, *New Phytologist* 2009, **182**,
- 6 799-816.
- 7 (4) J.R. Prohaska, *Am. J. Clin. Nutr.* 2008, **88**, 826S-829S.
- 8 (5) C.-N. Lok, C.-M. Ho, R. Chen, Q.-Y. He, W.-Y. Yu, H.
- 9 Sun, H. P. K.-H. Tam, J.-F. Chiu, and C.-M. Che, *J. Biol.*
- 10 *Inorg. Chem.* 2007, **12**, 527-534.
- 11 (6) M. C. Fung, and D. L. Bowen, *J. Toxicol. Clin. Toxicol.*
- 12 1996, **34**, 119-126.
- 13 (7) M. Trop, M. Novak, S. Rodl, B. Hellbom, W. Kroell, and
- 14 W. Goessler, *J. Trauma* 2006, **60**, 648-652.
- 15 (8) A. Changela, K. Chen, J. Holschen, C.E. Outten, T.V.
- 16 O'Halloran, and A. Mondragon, *Science* 2003, **301**, 1383-
- 17 1387.
- 18 (9) J.V. Stoyanov, J.L. Hobman, and N.L. Brown, *Mol.*
- 19 *Microbiol.* 2001, **39**, 502-512.
- 20 (10) J.A. Delmar, C.-C. Su, and E.W. Yu, *Biometals* 2013, **26**,
- 21 593-607.
- 22 (11) S. Franke, G. Grass, C. Rensing, and D.H. Nies, *J.*
- 23 *Bacteriol.* 2003, **185**, 3804-3812.
- 24 (12) E.-H. Kim, C. Rensing, and M.M. McEvoy, *Nat. Prod.*
- 25 *Rep.* 2010, **27**, 711-719.
- 26 (13) C. Rensing, and G. Grass, *FEMS Microbiol. Rev.* 2003,
- 27 **27**, 197-213.
- 28 (14) T.K. Janganan, V.N. Bavro, L. Zhang, D. Matak-
- 29 Vinkovic, N.P. Barrera, C. Venien-Bryan, C.V. Robinson,
- 30 M.I. Borges-Walmsley, and A.R. Walmsley, *J. Biol.*
- 31 *Chem.* 2011, **286**, 26900-26912.
- 32 (15) C.-C. Su, F. Long, M.T. Zimmermann, K.R. Rajashankar,
- 33 R.L. Jernigan, and E.W. Yu. *Nature* 2011, **470**, 558-563.
- 34 (16) C.-C. Su, F. Yang, F. Long, D. Reyon, M.D. Routh, D.W.
- 35 Kuo, A.K. Mokhtari, J.D.V. Ornam, K.L. Rabe, J.A. Hoy,
- 36 Y.J. Lee, K.R. Rajashankar, and E.W. Yu, *J. Mol. Biol.*
- 37 2009, **393**, 342-355.
- 38 (17) T.D. Mealman, M. Zhou, T. Affandi, K.N. Chacón, M.E.
- 39 Aranguren, N.J. Blackburn, V.H. Wysocki, and M.M.
- 40 McEvoy, *Biochem.* 2012, **51**, 6767-6775.
- 41 (18) I. Bagai, W. Liu, C. Rensing, N.J. Blackburn, and M.M.
- 42 McEvoy, *J. Biol. Chem.* 2007, **282**, 35695-35702.
- 43 (19) M.N. Ucisik, D.K. Chakravorty, and J.K.M. Merz,
- 44 *Biochem.* 2013, **52**, 6911-6923.
- 45 (20) I.R. Loftin, S. Franke, S.A. Roberts, A. Weichsel, A.;
- 46 Heroux, W.R. Montfort, C. Rensing, and M.M. McEvoy,
- 47 *Biochem.* 2005, **44**, 10533-10540.
- 48 (21) I.R. Loftin, N.J. Blackburn, and M.M. McEvoy, *J. Biol.*
- 49 *Inorg. Chem.* 2009, **14**, 905-912.
- 50 (22) T. Padilla-Benavides, A.M. George, M.M. McEvoy, and
- 51 J.M. Arguello, *J. Biol. Chem.* 2014, **289**, 20492-20501.
- 52 (23) K.N. Chacón, T.D. Mealman, M.M. McEvoy, and N.J.
- 53 Blackburn, *Proc. Nat. Acad. Sci.* 2014, **111**, 15373-15378.
- 54 (24) I. Bagai, C. Rensing, N.J. Blackburn, and M.M. McEvoy,
- 55 *Biochem.* 2008, **47**, 11408-11414.
- 56 (25) T.D. Mealman, I. Bagai, P. Singh, D.R. Goodlett, C.
- 57 Rensing, H. Zhou, V.H. Wysocki, and M.M. McEvoy,
- 58 *Biochem.* 2011, **50**, 2559-2566.
- 59 (26) G. Jeschke, R.J.M. Abbott, S.M. Lea, C.R. Timmel, and
- 60 J.E. Banham, *Angew. Chem. In. Ed.* 2006, **45**, 1058-1061.
- (27) B. Joseph, V.M. Morkhov, M. Yulikov, G. Jeschke, and
- E. Bordignon, *J. Biol. Chem.* 2014, **289**, 3176-3185.
- (28) G. Jeschke, *Annu. Rev. Phys. Chem.* 2012, **63**, 419-446.
- (29) G. Sicoli, G. Mathis, O. Delalande, Y. Boulard, D.
- Gasparutto, and S. Garnbarelli, *Angew. Chem. In. Ed.*
- 2008, **47**, 735-737.
- (30) P. Zou, and H.S. Mchaourab, *Biophys. J.* 2010, **98**, L18-
- L20.
- (31) I.D. Sahu, B.M. Kroncke, R. Zhang, M.M. Dunagan, H.J.
- Smith, A. Craig, R.M. McCarrick, C.R. Sanders, and G.A.
- Lorigan, *Biochem.* 2014, **53**, 6391-6401.
- (32) M.C. Puljung, H.A. DeBerg, W.N. Zagotta, and S. Stoll,
- Proc. Nat. Acad. Sci.* 2014, **111**, 9816-9821.
- (33) A.D. Milov, Yu.D. Tsvetkov, F. Formaggio, S. Oancea, C.
- Toniolo, and J. Raap, *J. Phys. Chem. B* 2003, **107**, 13719-
- 13727.
- (34) M. Pannier, S. Veit, A. Godt, G. Jeschke, and H.W.
- Spiess, *J. Magn. Res.* 2000, **142**, 331-340.
- (35) R.G. Larsen, and D.J. Singel, *J. Chem. Phys.* 1993, **98**,
- 5134-5146.
- (36) C. Altenbach, A.K. Kusnetzow, O.P. Ernst, K.P.
- Hofmann, and W.L. Hubbell, *Proc. Nat. Acad. Sci.* 2008,
- 105**, 7439-7444.
- (37) Q. Cai, A.K. Kusnetzow, W.L. Hubbell, I.S. Haworth,
- G.P.C. Gacho, N. Van Eps, K. Hideg, E.J. Chambers, and
- P.Z. Qin, *Nucl. Acids Res.* 2006, **34**, 4722-4730.
- (38) W.L. Hubbell, A. Gross, R. Langen, and M.A. Lietzow,
- Curr Opin Struc Biol* 1998, **8**, 649-656.
- (39) H.S. Mchaourab, K.J. Oh, C.J. Fang, and W.L. Hubbell,
- Biochem.* 1997, **36**, 307-316.
- (40) W.L. Hubbell, H.S. Mchaourab, C. Altenbach, and M.A.
- Lietzow, *Structure* 1996, **4**, 779-783.
- (41) G. Jeschke, *Prog. Nuc. Magn. Reson. Spec.* 2013, **72**, 42-
- 60.
- (42) Y. Xue, A.V. Davis, G. Balakrishnan, J.P. Stasser, B.M.
- Staehlin, P. Focia, T.G. Spiro, J.E. Penner-Hahn, and T.V.
- O'Halloran, *Nat. Chem. Biol.* 2008, **4**, 107-109.
- (43) R.K. Saiki, D.H. Gelfand, S. Stoffel, S.J. Scharf, R.
- Higuchi, G.T. Horn, K.B. Mullis, and H.A. Erlich, *Science*
- 1988, **239**, 487-491.
- (44) W. Don, S.G. Fischer, M.W. Kirschner, and U.K.
- Laemmli, *J. Biol. Chem.* 1971, **252**, 1102-1106.
- (45) G.L. Peterson, *Anal. Biochem.* 1997, **83**, 346-356.
- (46) G. Jeschke, *Bio. Magn. Reson.* 2007, **27**, 287-288.
- (47) A.R. Levy, V. Yarmiyayev, Y. Moskovitz, and S.
- Ruthstein, *J. Phys. Chem. B* 2014, **118**, 5832-5842.
- (48) Y. Shenberger, V. Yarmiyayev, and S. Ruthstein, *S. Mol.*
- Phys.* 2013, **111**, 2980-2991.
- (49) J.T. Rubino, P. Riggs-Gelasco, and K.J. Franz, *J. Biol.*
- Inorg. Chem.* 2010, **15**, 1033-1049.
- (50) J. Jiang, I.A. Nadas, K.M. Alison, and K.J. Franz, K. J.
- Inorg. Chem.* 2005, **44**, 9787-9794.